Theoretical Analysis on the Fundamental and Overtone OH Stretching Spectra of Several Simple Acids and Alcohols

Kaito Takahashi, Michihiko Sugawara, and Satoshi Yabushita*

Department of Chemistry, Faculty of Science and Technology, Keio University, 3-14-1 Hiyoshi, Kohoku-ku, Yokohama, 223-8522 Japan

Received: March 18, 2003; In Final Form: September 29, 2003

We calculated the fundamental and overtone OH stretching vibrational spectra for the following alcohols and acids—methanol, ethanol, 1-propanol, 2-propanol, *tert*-butyl alcohol, 2,2,2-trifluoroethanol, acetic acid, trifluoroacetic acid, and nitric acid—under the local mode model. We obtained the potential energy surface (PES) and the dipole moment function (DMF) by hybrid density functional theory method and performed vibrational calculation using the grid variational method. The theoretical results were in good agreement with the experimental observations. It was found that the molecular shape, such as the rotational conformation, is very important in the description of the OH stretching vibrational spectra. For alcohols with rotational conformers, such as ethanol, 1-propanol, and 2-propanol, we found that the isomer with the alkyl group in the trans position of the vibrating OH bond has a larger transition energy and a slightly stronger absorption intensity. We analyzed the first and second derivative terms of the DMF of these molecules to obtain insight on the difference in the absorption intensities. In addition, for the fundamental spectra, we investigated the difference between the local and normal mode vibrational calculation results.

1. Introduction

Recent advances in experimental techniques enable one to observe the details of stretching overtone spectra of XH bonds where X = C, O, and so on. In treating these overtone transitions, the local mode model, in which the vibrational wave function is described as a product of anharmonic oscillators using internal coordinates, has shown great success.[1−7] Therefore, one is able to obtain insight into the individual XH bonds from the interpretation of these overtone spectra. Quantum chemical calculations have helped rationalize several interesting observations in overtone spectroscopy.[5−9] For example, we have reported that the difference in the absorption intensity of the CH stretching vibration between the trans and cis isomer of 1,2-dichloroethylene is due to the difference in the second derivative term of the dipole moment function (DMF).[7]

The OH stretching overtone spectra have been studied with great interest in atmospheric studies.[10−12] For example, overtone absorption by water clusters is thought to account for the difference between the modeled and the observed absorption of sun light by the atmosphere.[11] However, obtaining the experimental absorption intensity for each cluster, for example, dimer, trimer, and so on, is difficult. Furthermore, it is reported that overtone-initiated photodissociation processes are related to the production of atmospheric radicals in the lower stratosphere at high zenith angles.[12] Recently, Reynard and Donaldson have measured the $v = 3-5$ OH stretching overtone spectra of trifluoroacetic acid and have performed theoretical analysis of the overtone-initiated reactions on this molecule.[13] The knowledge of accurate absorption intensities on these transitions is important in understanding the significance of these processes in the atmosphere.

With the intent to identify the variations in OH vibrational absorption intensity from compound to compound and to ultimately arrive at an understanding of the substituent effect, Phillips et al. measured the fundamental and the first three overtones of the OH stretching vibrational spectra for the following eight molecules: methanol, ethanol, 1-propanol, 2-propanol, *tert*-butyl alcohol, 2,2,2-trifluoroethanol, acetic acid, and nitric acid.[14] In their work, the existence of two (or more) conformers was observed as multiplets in the absorption spectra of ethanol, 1-propanol, and 2-propanol. Upon the experimental analysis on the observed spectra of these alcohols with rotational conformers, they reported the band center of these multiplets for the peak position and integrated all of the conformer bands; thus, reported the total intensity for all of the conformers. Because it is difficult to assess the experimental absorption strength of each individual rotational conformer, theoretical calculations on these molecules will help further analysis on the observed spectra.

In the present work, we calculate the peak positions and the absorption intensities of the OH stretching spectra for the nine molecules mentioned above, under the local mode model. For 2,2,2-trifluoroethanol, ethanol, 1-propanol, and 2-propanol, we calculate the spectra for all of the possible rotational conformations. In addition, for the fundamental transitions, we perform comparisons with the values calculated from the normal mode model.

2. Theory and Computational Method

In the present calculation, we considered the local mode model,[1−7] in which only the stretching motion of the OH bond is taken into account. Thereby, we solved the Schrödinger equation for one-dimensional molecular vibration

$$H\psi_v(r) = \left[-\frac{\hbar^2}{2m_d}\frac{d^2}{dr^2} + V(r)\right]\psi_v(r) = E_v\psi_v(r) \qquad (1)$$

where m and $V(r)$ are the reduced mass of OH and the PES,

* To whom correspondence should be addressed. E-mail: yabusita@chem.keio.ac.jp. Fax: +81-45-566-1697.

10.1021/jp0346965 CCC: $25.00
Published on Web 11/12/2003

respectively. In other words, the PES in the present vibrational calculation is the OH potential curve.

We calculated the integrated absorption coefficient(km mol^{-1}, base *e*) of each OH stretching transition by

$$A(\upsilon) = \ln 10 \int \epsilon(\tilde{\nu}) d\tilde{\nu} = \frac{8N_A\pi^3}{300\,000hc}|\vec{\mu}_{0\upsilon}|^2\tilde{\nu}_{0\upsilon} = 2.506\,639\,488|\vec{\mu}_{0\upsilon}|^2\tilde{\nu}_{0\upsilon} \quad (2)$$

where $\epsilon(\tilde{\nu})$ is the molar extinction coefficient(base 10), $\tilde{\nu}_{0\upsilon}$ is the transition energy in cm^{-1}, and $|\vec{\mu}_{0\upsilon}|^2$ is the sum of the squared transition moment of the *x*, *y*, and *z* component in debye^2 unit

$$A(\upsilon) = 2.506\,639\,488\{[\int \psi_0(r)\mu_x(r)\psi_\upsilon(r)\,dr]^2 + [\int \psi_0(r)\mu_y(r)\psi_\upsilon(r)\,dr]^2 + [\int \psi_0(r)\mu_z(r)\psi_\upsilon(r)\,dr]^2\}\tilde{\nu}_{0\upsilon} \quad (3)$$

where $\psi(r)$ is the OH stretching wave function and $\mu(r)$ is the DMF of the respective direction. The values of the integrated absorption coefficient, *A*, which is given using the units km mol^{-1} throughout this paper, can be converted to the units cm molecule^{-1} (base e) and to dimensionless oscillator strengths by 1.66×10^{-19} cm molecule^{-1} mol km $^{-1} \times A$ and 1.87×10^{-7} mol km $^{-1} \times A$, respectively.

All of the quantum chemical calculations were performed using the hybrid density functional theory method using the B3LYP[15,16] functional with the 6-311++G(3df,3pd)[17−20] basis set on the Gaussian 98 program.[21] We took the OH bond as the *z* axis, with O as the origin and the atom bonded to the OH bond was placed in the *xz* plane. We performed geometry optimization for all of the molecules to obtain the equilibrium structure and then single-point calculations to obtain the PES and DMF. The latter calculations were done for every 0.1 Å OH bond length between the regions $r_{eq} - 0.5$ Å to $r_{eq} + 0.8$ Å and with two additional points at $r_{eq} \pm 0.05$ Å. All of the remaining molecular coordinates were kept at the calculated equilibrium values. The zero-point vibration energy for each molecule was calculated using the harmonic approximation. All of the calculated single-point results are given as additional information.

Using the 16 single-point calculation results mentioned above, we constructed the PES and DMF by sixth-order divided difference interpolation.[22,23] The vibrational calculations using these functions were done by the grid variational method.[24,25] We used 246 grid points between the range of $r_{eq} - 0.5$ Å to $r_{eq} + 0.8$ Å and the fifth-order finite difference approximation for the expression of the kinetic energy term. All of these calculations were done with *Mathematica*, and the accuracy of this method is discussed in our previous paper.[7]

3. Results and Discussions

In the following, we will report the calculated vibrational spectra for the nine molecules mentioned in the Introduction, as well as for the OH radical.

3.1. Geometry Optimization. As noted earlier, several alcohols calculated in the present study have rotational isomers, as shown in Figures 1 and 2.[26] The conformations of these alcohols can be named according to the different dihedral angles, where trans (t) is near 180°, gauche (g) is near 60°, and gauche′ (g′) is near −60°, respectively. In Figure 1, we show two molecules, namely, ethanol (2,2,2-trifluoroethanol has the same shape) and 2-propanol, with two different conformations, depending on the dihedral angle H1O1C1C2. As for 1-propanol, there are five distinctive conformers depending on the dihedral angles H1O1C1C2 and O1C1C2C3. In Figure 2, they are labeled using T, G, G′ and t, g, g′, the capital letter stands for the trans, gauche, or gauche′ relationship between the O1H1 and C1C2 bonds along the C1O1 bond, whereas the lower case letter

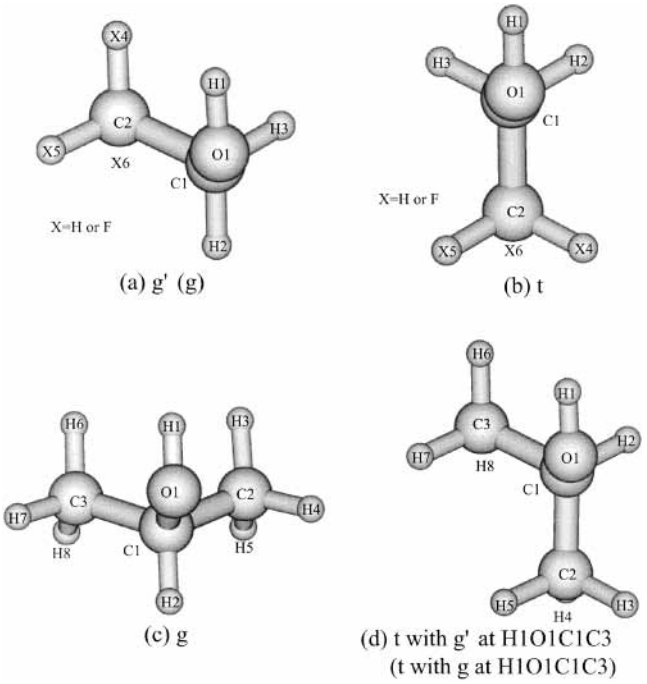

Figure 1. Schematic diagram of (a) *gauche*- and (b) *trans*-ethanol (2,2,2-trifluoroethanol) and (c) gauche- and (d) *trans*-2-propanol, drawn by the MOLDEN 3.6 program of ref 26. The labeling for the mirror images, i.e., conformational enantiomers, is given in parentheses.

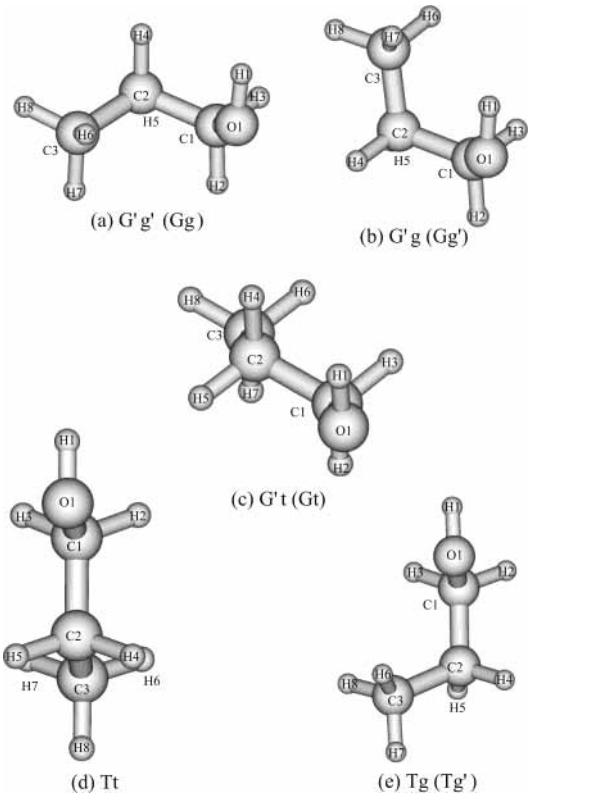

Figure 2. Schematic diagram of (a) *Gauche′ gauche′*-, (b) *Gauche′ gauche*-, (c) *Gauche′ trans*-, (d) *Trans trans*-, and (e) *Trans gauche*-1-propanol, drawn by the MOLDEN 3.6 program of ref 26. The labeling for the mirror images, i.e., conformational enantiomers, is given in parentheses.

TABLE 1: Relative Energies of the Conformers (kcal mol^{-1}) and Their Percentage Based on the Boltzmann Distribution (298 K) for 2,2,2-Trifluoroethanol, Ethanol, and 2-Propanol

	trifluoroethanol		ethanol		2-propanol	
	trans[a]	gauche[a]	trans[a]	gauche[a]	trans[a]	gauche[a]
energy	1.58	0.00	0.00	0.0984	0.00	0.214
percentage	3.4	96.4	37.2	62.8	73.0	27.0

[a] See Figure 1 for structure.

TABLE 2: Relative Energies of the Conformers (kcal mol^{-1}) and Their Percentage Based on the Boltzmann Distribution (298 K) for 1-Propanol

	1-propanol				
	Tt[a]	G't[a]	Tg[a]	G′g′[a]	G′g[a]
energy	0.00	0.0507	0.0591	0.194	0.286
percentage	13.7	25.1	24.7	19.7	16.9

[a] See Figure 2 for structure.

signifies the relationship between the O1C1 and the C2C3 bonds along the C1C2 bond. For conformations where mirror images, i.e., conformational enantiomers, exist, their labels are given in parentheses both in Figures 1 and 2. Upon comparison with Phillips' results, we took the Boltzmann distribution average intensity for the two (or more) conformers, under the assumption that the experiment was performed at room temperature (298 K).[27] Therefore, we calculated the relative percentage of abundance using the Boltzmann formula

$$\frac{N_i}{N_j} = \frac{g_i}{g_j} \exp\left(-\frac{E_i - E_j}{kT}\right) \tag{4}$$

where N_i/N_j is the population ratio of the two conformations, g_i/g_j is the ratio of the degeneracy, i.e., the number of enantiomers, and E_i and E_j are the total energies of the two conformers, respectively. The total energy for each conformer was obtained by adding the zero-point vibration energy to the electronic energy at each potential minimum. We multiplied this percentage with its respective calculated absorption intensity and summed for all conformations to obtain the Boltzmann average intensity. As for the peak position, we took the average value of the conformers, as done in the experimental analysis.[14] In Table 1, we report the relative energies of the two isomers along with the percentage calculated from the Boltzmann distribution for 2,2,2-trifluoroethanol, ethanol, and 2-propanol. The listed values have already been multiplied by their respective degeneracy. Therefore, although *trans*-ethanol is the lower energy conformation, *gauche*-ethanol has predominant intensity at room temperature due to its doubly degeneracy. In Table 2, we list the relative energies and the percentage for the five distinctive conformations of 1-propanol. For 2,2,2-trifluoroethanol, mostly one isomer, namely the gauche isomer, was calculated to be present at room temperature. This is in accord with Phillips' observation that only one band was observed for this molecule.[14] For ethanol, several experimental papers have reported that the trans isomer is slightly more stable than the gauche isomer. Kakar and Quade have measured an energy difference of 0.118 kcal mol^{-1} using microwave spectroscopy,[28] and Durig et al. have reported a value of 0.314 kcal mol^{-1} using gas-phase Raman spectroscopy,[29] whereas Fang and Swofford have reported a value of 0.7 kcal mol^{-1} from overtone spectroscopy.[30] As for theoretical calculations, Schäfer et al. have reported that the trans isomer is stable by 0.1 kcal mol^{-1} using the Hartree−Fock method with the 4-21G basis set.[31] Recently, Swofford et al. have reported that the trans isomer is stable by about 0.32 and 0.33 kcal mol^{-1} from theoretical calculations using the MP2 and CCD methods with the 6-311++G** basis set, respectively.[32] We obtained an energy difference of 0.0984 kcal mol^{-1} in favor of the trans isomer.

TABLE 3: Harmonic and Anharmonic Terms (cm^{-1}) of Acids and Alcohols[a] along with the Calculated and Experimental Bond Length of the OH Bond (Å)

	calcd				expt		
	ω_e	$\chi_e\omega_e$	r_{eOH}[c]	r_{0OH}[d]	ω_e[e]	$\chi_e\omega_e$[e]	r_{OH}
O_2NOH	3712	72.7	0.9709	0.9877	3707	79	0.9640[f]
CF_3COOH	3742	76.7	0.9689	0.9855	3749	82	
CH_3COOH	3751	77.6	0.9679	0.9846	3747	83.1	
CF_3CH_2OH	3814	78.6			3826	84.2	
gauche[b]	3814	78.6	0.9622	0.9787			
trans[b]	3846	78.6	0.9601	0.9764			
CH_3OH	3837	79.9	0.9600	0.9765	3853	85	0.956[g]
CH_3CH_2OH	3827	79.8			3836	84.8	
gauche[b]	3819	80.1	0.9612	0.9778			
trans[b]	3835	79.6	0.9604	0.9768			0.9710[h]
$CH_3CH_2CH_2OH$	3829	79.9			3842	86.1	
Tt[b]	3836	79.8	0.9602	0.9767			
G't[b]	3820	80.1	0.9612	0.9777			
Tg[b]	3840	79.7	0.9600	0.9764			
G′g′[b]	3818	80.2	0.9613	0.9778			
G′g[b]	3832	79.8	0.9605	0.9769			
$(CH_3)_2CHOH$	3811	80.0			3827	86	
gauche[b]	3803	80.0	0.9625	0.9791			
trans[b]	3821	79.9	0.9612	0.9777			
$(CH_3)_3COH$	3811	80.0	0.9620	0.9785	3818	86.5	
OH	3709	73.5	0.9739	0.9905	3735	82.5	0.9677[i]

[a] For alcohols with conformers, the average value is listed except for 2,2,2-trifluoroethanol. [b] Values for each rotational conformer. See Figures 1 and 2 for the labeling on the structure. [c] Equilibrium bond length. [d] Bond length including the zero-point correction. [e] Experimental results from ref 14, except for CF_3COOH which is from ref 13 and OH which is from ref 35. [f] Experimental data on the substitution structure (r_s) from ref 36. [g] Experimental data from ref 37. [h] Experimental data from ref 38. [i] Experimental data on the equilibrium bond length (r_e) from ref 39.

For ethanol, 1-propanol, and 2-propanol, one should compare the experimental results with the calculated average values for the transition energy and the calculated Boltzmann average values for the absorption intensity. As for 2,2,2-trifluoroethanol, the calculation results for the gauche isomer should be compared with experimental results. In the tables, we will also report the results for each isomer and compare the difference between them in the latter portion of this section.

3.2. Vibrational Calculation Results on the Transition Energies of the Alcohols and Acids. It is known that, under the local mode picture, the transition energies of XH stretching vibration fit the Birge−Sponer relationship $\tilde{\nu}_{v0} = Av - Bv^2$.[30] This expression is related to the harmonic and anharmonic terms of a Morse oscillator by $\omega_e = A + B$ and $\omega_e\chi_e = B$. These terms were used by Phillips et al. to compare the molecules.[14] In Table 3, we list the harmonic and anharmonic terms calculated from the Birge−Sponer plot of our theoretical energies for the $v = 1-4$ excitations for all of the alcohols (same way as the experimental results[14]). For acetic acid, because Phillips' experimental results were present only for $v = 1-3$, we used the calculation results of $v = 1-3$ to obtain the two terms. For nitric acid, Phillips et al. reported values given by Donaldson et al.,[33] which were obtained by fitting experimental results of $v = 1-6$; thus, we performed the fitting with the same number of calculated results. For trifluoroacetic acid, Reynard and Donaldson obtained the two terms by fitting their overtone results ($v = 3$ and 4) along with Kagarise's experimental result on the fundamental transition;[34] thus, we used the respective

TABLE 4: Transition Energies (cm^{-1}) and Integrated Absorption Coefficients (km mol^{-1}) for the Fundamental Transition of Alcohols and Acids Based on Two Different PESs and DMFs: Anharmonic PES and Nonlinear DMF (anharm PES n−l DMF), Anharmonic PES and Linear DMF (anharm PES lin DMF), Harmonic PES and Nonlinear DMF (harm PES n−l DMF), and Harmonic PES and Linear DMF (harm PES lin DMF), Calculated under the Local Mode Model

			calcd						
			anharm PES				harm PES		
	expt[b]			n−l DMF		lin DMF		n−l DMF	lin DMF
	$\tilde{\nu}_{10}$	A	$\tilde{\nu}_{10}$	A	A_z[c]	A	$\tilde{\nu}_{10}$	A	A
O_2NOH	3551	56.9	3569	85.4	75.7	86.2	3729	89.4	88.4
CF_3COOH	3587		3589	74.7	68.9	77.9	3752	79.8	80.0
CH_3COOH	3581	52.6	3596	44.5	42.4	48.4	3759	49.0	49.7
CF_3CH_2OH	3657	34.5	3657	36.2	32.9	40.4	3824	40.7	41.5
gauche[a]			3657	36.2	32.9	40.4	3824	40.7	41.5
trans[a]			3689	39.8	36.8	45.4	3854	45.4	46.6
CH_3OH	3681	19.7	3678	19.1	17.5	23.6	3846	23.6	24.3
CH_3CH_2OH	3665	16.4	3668	14.0	12.4	18.0	3836	17.8	18.4
gauche[a]			3659	13.2	11.3	16.8	3828	16.8	17.2
trans[a]			3677	15.3	14.5	19.9	3844	19.5	20.4
$CH_3CH_2CH_2OH$	3669	15.4	3670	14.7	13.2	18.9	3839	18.7	19.4
Tt[a]			3678	15.2	14.6	20.0	3846	19.7	20.6
G't[a]			3660	13.5	11.3	17.4	3829	17.3	17.8
Tg[a]			3681	17.2	16.4	22.4	3849	21.9	22.9
G′g′[a]			3659	13.8	11.8	17.6	3828	17.5	18.1
G′g[a]			3673	13.2	11.9	16.7	3841	16.4	17.1
$(CH_3)_2CHOH$	3655	11.8	3652	9.25	7.88	11.9	3821	11.8	12.2
gauche[a]			3641	9.28	7.57	9.85	3810	9.77	10.1
trans[a]			3663	9.24	7.99	12.7	3832	12.5	13.0
$(CH_3)_3COH$	3644	9.27	3651	5.98	4.59	9.65	3818	8.57	9.91
OH	3570		3562	11.8	11.8	12.5	3718	12.8	12.8

[a] Values for each rotational conformer. See Figures 1 and 2 for the labeling on the structure. [b] Experimental results from ref 14, except for CF_3COOH which is from ref 34 and OH which is from ref 35. [c] The absorption intensity calculated from only the z component of the transition moment.

calculation results for the fitting. For the two terms of OH radical, we fitted the experimental values for the $\upsilon = 1-3$ transitions given by Mantz et al.;[35] therefore, the corresponding calculated values were used in the fitting. We also listed the calculated OH bond length (for molecules with rotational conformers, all values are listed), both the equilibrium bond length r_{eOH} and that with zero-point correction r_{0OH}, and the available experimental OH bond lengths for nitric acid,[36] methanol,[37] *trans*-ethanol,[38] and the OH radical.[39] It can be seen that, whereas the harmonic terms show errors of less than 1%, the anharmonic terms were underestimated by 10 percent. The same trend was seen in our previous calculation on 1,2-dichloroethylene and can be understood as a limitation of the current hybrid density functional theory method. However, the calculated values reproduced two characteristic experimental trends reported by Phillips et al.[14] First, compared to the alcohols, the two acids have lower values for both harmonic and anharmonic terms. Second, the anharmonic terms for the nonhalogenated alcohols are nearly equal (bottom five molecules but the OH radical in Table 3), whereas the harmonic terms tend to decrease with the size of the organic substituents. Fang and Compton have also reported that the experimental harmonic term of primary alcohols such as methanol and 1-propanol is approximately 20 cm^{-1} larger than the one of 2-propanol, which is 40 cm^{-1} larger than the one of *tert*-butyl alcohol.[40] In addition, we are able to see that the harmonic terms, both the observed and the calculated, are inversely correlated to the calculated OH bond lengths. This is in accord with Henry's bond length frequency correlation relationship.[41] As for the comparison with experimental bond lengths, although there exists some difference for *trans*-ethanol, the same trend can also be seen between the bond length and the transition energies. As for the OH bond length in *trans*-ethanol, Swofford et al. have also reported that the calculated value is underestimated by 0.01 Å.[32] It can be noticed that, compared to the results of the OH radical, the transition energies of the alcohols and acids are greater, signifying that the OH bond is strengthened in a polyatomic molecule.

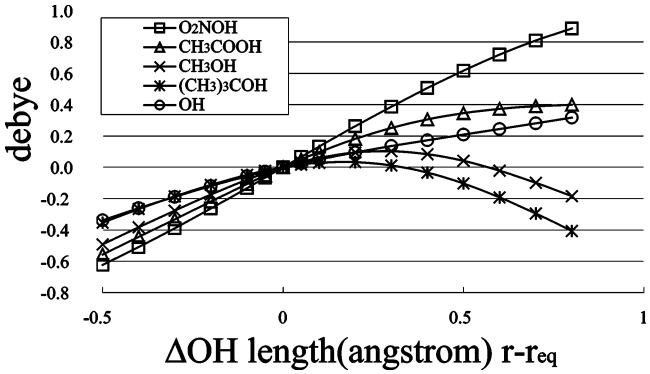

Figure 3. Deviation of the z component of the dipole moment function of nitric acid, acetic acid, methanol, *tert*-butyl alcohol, and the OH radical.

3.3. Vibrational Calculation Results on the Fundamental Transition of Alcohols and Acids. In Table 4, we compared the calculated and the observed peak position and absorption intensity for the fundamental transitions. For the alcohols with rotational conformers, we reported the average value in the first row and the values for each conformer below it. First, we will examine the fully numerical results calculated using the interpolated PES and DMF, labeled as "anharm PES n−l DMF", and the experimental results. One should note that this PES includes anharmonic terms and that this DMF includes all of the nonlinear terms. As mentioned by Phillips,[14] the fundamental absorption intensity increases with the electron withdrawing ability of the adjacent substituent bonded to the OH bond. Upon the division of the absorption intensity into x, y, and z components following eq 3, it was found that the dominant contribution to the intensity of the fundamental transition arises from the component of the dipole moment parallel to the OH

TABLE 5: Transition Energy (cm^{-1}) and the Integrated Absorption Coefficient (km mol^{-1}) for the Fundamental Transitions of Alcohols and Acids Calculated under the Normal Mode Model[a]

	$\tilde{\nu}_{10}$	A		$\tilde{\nu}_{10}$	A
O_2NOH	3726	94.4	CH_3CH_2OH[c]	3835	24.7
CF_3COOH	3748	95.1	$CH_3CH_2CH_2OH$[c]	3837	25.7
CH_3COOH	3754	60.7	$(CH_3)_2CHOH$[c]	3820	18.7
CF_3CH_2OH[b]	3822	48.5	$(CH_3)_3COH$	3818	14.2
CH_3OH	3846	30.5	OH	3719	12.8

[a] The results from Gaussian 98. [b] The value for the gauche isomer is listed. [c] The average value for the conformers is listed for the transition energy while the Boltzmann average is listed for the intensity.

bond, the *z* direction in the present work (Table 4, column 6). In Figure 3, we plot the deviation of the *z*-DMF (the equilibrium value is offset to zero for all the molecules) for nitric acid, acetic acid, methanol, *tert*-butyl alcohol, and the OH radical. We compared these molecules, because the values for the molecules with two or more conformers are hard to compare. In the latter section of this paper, we will examine the differences in the DMF of the alcohols with conformers. As can be seen from Figure 3, the *z* component of the DMF is steeper and less curved for the molecules with greater electron withdrawing substituent. This trend is fairly similar to the one-dimensional DMF that Phillips et al. determined by empirical fitting.[14] Another interesting observation is that the DMF of the OH radical acts as a dividing line between the acids and the alcohols.

In addition to these results, in Table 4, we list the local mode results obtained by approximating the PES as a quadratic function and the DMF as a linear function. This is labeled as "harm PES lin DMF" in columns 8 and 10. To obtain the harmonic PES, we first performed additional single-point calculations for $r_{eq} \pm 0.01$ Å and $r_{eq} \pm 0.02$ Å. Using these results along with the one for r_{eq}, we obtained the second derivative of the potential energy by five-point numerical differentiation. The first derivative of the dipole moment was obtained from the analytical calculation results of the atomic polar tensors given in the output of the Gaussian 98 program.[21] It can be easily found that the harmonic approximation, owing to the neglecting of the anharmonic term in the PES, overestimates the observed peak position. Also, one can notice that the "harm PES lin DMF" approximation sometimes overestimates the absorption intensity. Because the "anharm PES n−l DMF" calculation results reproduce the experimental values in general, this deviation is the result of neglecting the higher order terms in the PES and DMF. As seen in columns 7 and 9 of Table 4, the results on the absorption intensity using the combination of either anharmonic PES and linear DMF ("anharm PES lin DMF") or harmonic PES and nonlinear DMF ("harm PES n−l DMF") give values fairly similar to the ones given by harmonic PES and linear DMF. In other words, the nonlinearity of the DMF plays an important role only with the wave functions from the anharmonic PES, and the anharmonicity of the wave function alone causes a minimal effect when we neglect the nonlinearity of the DMF. This is easily understood from the selection rule for the harmonic wave functions. Compared to the "anharm PES n−l DMF" results, calculations using the linear DMF overestimate the absorption intensity due to the fact that the quadratic term of the DMF in the direction of the stretching bond usually takes the opposite sign of the linear term. This is because upon bond dissociation the absolute value of the DMF should terminate at a finite value rather than increase to infinity (Figure 3). This is true in all of the molecules calculated in the present work. As will be shown later, this difference in the sign of the first and second derivative causes the transition moment calculated from the nonlinear DMF to be smaller than the one calculated from the linear DMF alone for the wave functions calculated from the anharmonic PES.

Next, in Table 5, we will compare the local mode results mentioned above with the normal mode calculation results obtained by the Gaussian 98 program using the "Freq" keyword. Because the normal mode calculations employ the harmonic PES and linear DMF approximation, we will compare them with the local mode results calculated by the same approximation. In the local mode model, we considered that all of the freedom other than the OH bond length is at the equilibrium structure; however, this causes the center of mass to shift slightly as we deviate the OH bond length. In the normal mode coordinate, the shortening of the NO (for nitric acid) or CO (for all other acids and alcohols) bond is accompanied by the OH bond stretching. This additional deviation in the normal mode coordinate was very small and about 16 times (mass ratio)

TABLE 6: Calculated and Experimental[a] Values for the Integrated Absorption Coefficients (km mol^{-1}) of the Overtone Transitions of Alcohols and Acids

	A ($v = 2$)	A ($v = 3$)	A ($v = 4$)	A ($v = 5$)	A ($v = 6$)[c]
O_2NOH	3.14(2.00)	1.84×10^{-1}(1.75×10^{-1})	1.64×10^{-2}(1.69×10^{-2})	2.11×10^{-3}	3.51×10^{-4}
CF_3COOH	3.49	1.83×10^{-1}(1.63×10^{-1})	1.41×10^{-2}(1.01×10^{-2})	1.68×10^{-3}	2.74×10^{-4}
CH_3COOH	3.00(3.44)	1.74×10^{-1}(1.57×10^{-1})	1.36×10^{-2}	1.59×10^{-3}	2.55×10^{-4}
CF_3CH_2OH	2.83(2.32)	1.64×10^{-1}(1.10×10^{-1})	1.24×10^{-2}(0.76×10^{-2})	1.40×10^{-3}	2.15×10^{-4}
gauche[b]	2.83	1.64×10^{-1}	1.24×10^{-2}	1.40×10^{-3}	2.15×10^{-4}
trans[b]	3.52	1.95×10^{-1}	1.42×10^{-2}	1.59×10^{-3}	2.41×10^{-4}
CH_3OH	3.15(1.63)	1.95×10^{-1}(1.44×10^{-1})	1.45×10^{-2}(1.02×10^{-2})	1.60×10^{-3}	2.44×10^{-4}
CH_3CH_2OH	2.88(2.18)	1.84×10^{-1}(1.35×10^{-1})	1.36×10^{-2}(0.92×10^{-2})	1.47×10^{-3}	2.21×10^{-4}
gauche[b]	2.68	1.71×10^{-1}	1.27×10^{-2}	1.38×10^{-3}	2.07×10^{-4}
trans[b]	3.21	2.05×10^{-1}	1.51×10^{-2}	1.63×10^{-3}	2.46×10^{-4}
$CH_3CH_2CH_2OH$	2.94(2.64)	1.83×10^{-1}(1.25×10^{-1})	1.35×10^{-2}(0.84×10^{-2})	1.46×10^{-3}	2.20×10^{-4}
Tt[b]	3.52	2.19×10^{-1}	1.60×10^{-2}	1.75×10^{-3}	2.68×10^{-4}
G't[b]	2.76	1.75×10^{-1}	1.31×10^{-2}	1.42×10^{-3}	2.12×10^{-4}
Tg[b]	3.43	2.09×10^{-1}	1.51×10^{-2}	1.63×10^{-3}	2.45×10^{-4}
G'g'[b]	2.69	1.71×10^{-1}	1.24×10^{-2}	1.32×10^{-3}	1.95×10^{-4}
G'g[b]	2.30	1.45×10^{-1}	1.09×10^{-2}	1.22×10^{-3}	1.83×10^{-4}
$(CH_3)_2CHOH$	2.54(2.51)	1.66×10^{-1}(1.23×10^{-1})	1.23×10^{-2}(0.97×10^{-2})	1.33×10^{-3}	1.96×10^{-4}
gauche[b]	2.25	1.47×10^{-1}	1.09×10^{-2}	1.16×10^{-3}	1.74×10^{-4}
trans[b]	2.64	1.73×10^{-1}	1.28×10^{-2}	1.38×10^{-3}	2.04×10^{-4}
$(CH_3)_3COH$	2.23(1.35)	1.49×10^{-1}(1.23×10^{-1})	1.11×10^{-2}(1.02×10^{-2})	1.17×10^{-3}	1.73×10^{-4}
OH	6.46×10^{-1}	5.03×10^{-2}	4.74×10^{-3}	5.91×10^{-4}	9.43×10^{-5}

[a] The experimental values listed in the parenthesis are from ref 14, except for CF_3COOH which is from ref 13. [b] Values for each rotational conformer. See Figures 1 and 2 for the labeling on the structure. [c] From the examination on the convergence of these values, we report that they are accurate only to the first digit.

smaller than the deviation in the OH bond length for the molecules studied in this work. Furthermore, this difference in coordinates leads to a very small difference in the transition energies. However, as seen from the difference in the absorption intensities given in Table 4 (harm PES lin DMF) and Table 5, the dipole moment derivative results in a great increase. This is because in the molecules studied here the adjacent N or C atom has a relatively positive charge, and the decrease in the NO or CO distance accompanied by the OH bond stretching would cause an additional increase in the dipole moment parallel to the O(negative)H(positive) bond. It can also be noticed that the ratio between the normal mode and local mode absorption intensities increases as the electron withdrawing ability of the substituent decreases, i.e., as the positive charge of the substituents increases. As for the comparison with the experimental results, the normal mode results overestimate both the transition energy and the absorption intensity.

3.4. Vibrational Calculation Results on the Overtone Transition of Alcohols and Acids. The calculated and the experimental absorption intensities for the overtones are listed in Table 6. We applied the logarithmic deviation defined by Quack et al.[42] as

$$\Delta = \left\{ \frac{1}{n_{\mathrm{dat}}} \sum_{i=1}^{n_{\mathrm{dat}}} [\ln(A_i^{\mathrm{calc}}/A_i^{\mathrm{exp}})]^2 \right\}^{1/2} \quad (5)$$

to show the overall agreement between the calculated and the observed intensities. Compared to all of the data given by Phillips et al.[14] and the data on trifluoroacetic acid given by Reynard and Donaldson (for the experimental values on trifluoroacetic acid, we omitted the $v = 5$ results because the low precision for this value was mentioned in their paper[13]), we obtained a value of 0.307, signifying the high accuracy of the present calculation. As Phillips reported, there is no simple trend for the absorption intensities of the overtones.[14] The absorptions in the overtones are related to the anharmonicity in both the PES and the DMF, and because these effects are not simply additive, it is very hard to examine the origin of overtone intensity. It should be noted that both Medvedev[43] and Lehmann[44] have reported that the inner wall of the potential dominates the overtone intensity, although both used a DMF very similar to a linear function for their analysis.

In Figure 4, we separated the absorption intensity of the first three overtones into their *x*, *y*, and *z* terms, as in eq 3, for the five aforementioned molecules: nitric acid, acetic acid, methanol, *tert*-butyl alcohol, and OH radical. Because of symmetry reasons, the contribution of the *y* direction term is zero. It can be seen that the contribution of the *x* and *z* component in the overtone absorptions varies from molecule to molecule, thus, making it hard to perform further analysis on these five molecules. For example, for the acids, both the *x* and *z* components have a fairly large contribution, whereas for the alcohols, the contribution of the *z* component is about two times greater than that of the *x* component. From this result, we might conclude that the experimental analysis using a fit to a one-dimensional DMF is an unphysical way to investigate the overtone intensity. As Quack et al. have reported, such a one-dimensional DMF is an effective DMF and cannot be easily identified with the properties of the true DMF.[45] However, it should be noted that the empirical one-dimensional DMF can be understood as the function describing the dipole moment vector pointing a certain effective direction within the *xz* plane. For the molecules calculated here, this direction is within 30 degrees of the *z* axis. This is seen in the similar trends between

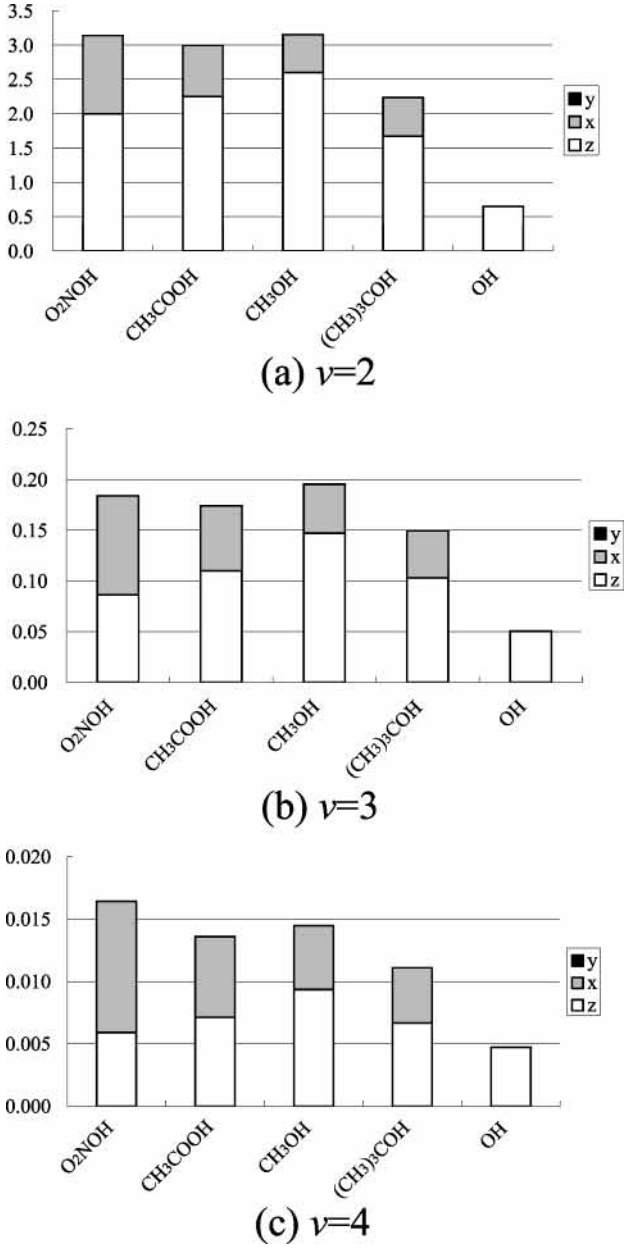

Figure 4. Separation of the absorption intensity of the (a) $v = 2$, (b) $v = 3$, and (c) $v = 4$ transition of nitric acid, acetic acid, methanol, *tert*-butyl alcohol, and the OH radical into the *x*, *y*, and *z* contributions.

the DMF in the direction parallel to the OH bond (*z*) and the one-dimensional DMF that Phillips et al. have reported.[14] Another point to notice is that the polyatomic molecules have very similar absorption intensities and the OH radical has exceptionally small intensities. For the overtone ($v = 3-5$) CH oscillator intensities, Burberry and Albrecht have reported the similarity among a wide range of liquid hydrocarbons.[46] We are presently performing further analysis to understand the origin of this "universal intensity concept" and to obtain the insight on the origin of overtone intensity in polyatomic molecules.

3.5. Differences in Transition Energies Between Rotational Conformers. In the following, we will examine the calculation results for the alcohols with rotational conformers. As seen in Table 3, the trans isomer (the alkyl substituent is in the trans position of the O1H1 bond along the C1O1 bond) of 2,2,2-trifluoroethanol, ethanol, and 2-propanol all have larger harmonic terms compared to their gauche counterpart. This is in accord with Fang's report that the high energy band within each

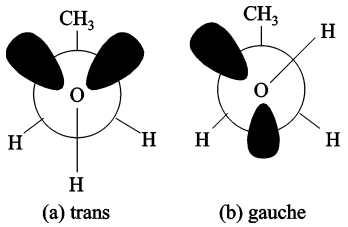

Figure 5. Schematic Newman projection of *trans*- and *gauche*-ethanol, indicating the position of the oxygen lone pair orbitals relative to the adjacent methylene hydrogens.

overtone region is assigned to the trans conformer for ethanol.[30,40] However, it is contradictory to his assignment on 2-propanol, where gauche was reported to be responsible for the high energy peak.[40] Xu et al. measured the $\upsilon = 3-5$ OH overtones of isobutyl alcohol and assigned them based on the density functional calculation results on the fundamental transition.[47] They also assigned the high energy peak to the rotational conformer with the alkyl group in the trans position of the OH bond.

Next, we will examine the results for the five conformers of 1-propanol. As seen in Table 3, the two isomers which have a trans configuration for the O1H1 and C1C2 (labeled by "T") have a slightly higher transition energy, just like the molecules mentioned above. Furthermore, for isobutyl alcohol, Xu et al. reported that within the isomer with the gauche conformation in H1O1C1C2 the conformer with the C-methyl bond parallel to the OH bond has the largest transition energy.[47] In the present study, the G′g conformer, which has this feature (see Figure 2), does indeed have the largest transition energy within the "G" conformation. On the other hand, the conformational change with respect to the dihedral angle of O1C1C2C3 does not cause a great difference in the transition energy between the two pairs Tt, Tg and G′t, G′g′.

From the above comparison, it may be concluded that experimental and theoretical results show that the rotational conformer with the alkyl group in the trans position of the stretching OH bond has a higher transition energy. Krueger and Wieser, who measured the fundamental absorption of the OH and α-CD bonds (the CD bond on the α-carbon, the carbon bonded to the vibrating OH bond) for CH_3CD_2OH, $(CH_3)_2$-CDOH, and $(CH_3)_2CDSH$, have reported that the increase in $\tilde{\nu}_{OH}$ and decrease in $\tilde{\nu}_{\alpha-CD}$ is related to the number of α-CD bonds in the trans position of the oxygen lone pair orbitals.[48] They explained this relationship by the delocalization of the lone pair orbitals on the oxygen atom into the σ^*_{CH} orbital of the adjacent carbon. According to their explanation, this increases the s character of the OH bond and strengthens the OH bond while it weakens the CH bond, thus, resulting in an increase in the $\tilde{\nu}_{OH}$ and a decrease in $\tilde{\nu}_{\alpha-CH}$. As seen in Figure 5, the trans isomer always has a greater number of CH bonds in the trans position of the lone pair orbitals, i.e., in the gauche position of the OH bond, thereby the transition energies of the OH vibration are greater. Similar explanations based on the delocalization of the lone pair electrons into the antibonding orbital have been used to explain the "no bond resonance", the "anomeric" or "gauche" effect, and "negative hyperconjugation".[49,50] We presently pursue the natural bond orbital analysis on the quantum chemical calculation results in order to clarify this feature.

3.6. Differences in Absorption Intensities Between Rotational Conformers. As seen in Tables 4 and 6, the intensities of the trans conformers (the position of the alkyl chain with respect to the OH bond) of 2,2,2-trifluoroethanol, ethanol, and 2-propanol are slightly stronger than its respective gauche conformers for each transition. In comparing the absorption intensities between the rotational conformers, it is logical to separate the transition moment into the *x*, *y*, and *z* contributions,

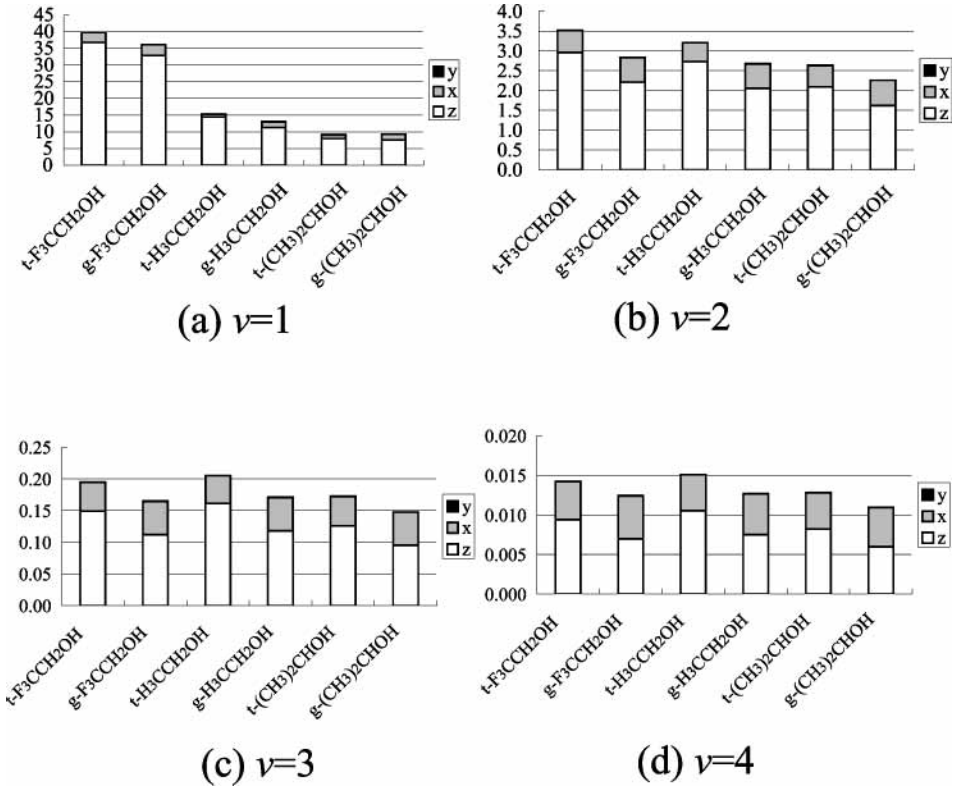

Figure 6. Separation of the absorption intensity of the (a) $\upsilon = 1$, (b) $\upsilon = 2$, (c) $\upsilon = 3$, and (d) $\upsilon = 4$ transition of ethanol, 2,2,2-trifluoroethanol, and 2-propanol into the *x*, *y*, and *z* contributions.

TABLE 7: Separation of the *z* Transition Moments (debye) of Ethanol into Their Dependence on the Linear and Nonlinear Terms of the Dipole Moment Function

v	R^1	R^2	R^3	R^4	sum $(R^1-R^4)^a$	calc(full)^b
			trans			
1	4.5×10^{-2}	-4.3×10^{-3}	-1.1×10^{-3}	7.8×10^{-5}	4.0×10^{-2}	4.0×10^{-2}
2	5.0×10^{-3}	6.9×10^{-3}	5.7×10^{-4}	-1.4×10^{-4}	1.2×10^{-2}	1.2×10^{-2}
3	9.8×10^{-4}	1.9×10^{-3}	-5.2×10^{-4}	5.1×10^{-5}	2.4×10^{-3}	2.5×10^{-3}
4	2.5×10^{-4}	5.9×10^{-4}	-2.7×10^{-4}	-2.9×10^{-5}	5.4×10^{-4}	5.4×10^{-4}
			gauche			
1	4.0×10^{-2}	-3.7×10^{-3}	-9.5×10^{-4}	7.4×10^{-5}	3.5×10^{-2}	3.5×10^{-2}
2	4.5×10^{-3}	5.9×10^{-3}	5.2×10^{-4}	-1.4×10^{-4}	1.1×10^{-2}	1.1×10^{-2}
3	8.7×10^{-4}	1.7×10^{-3}	-4.7×10^{-4}	4.8×10^{-5}	2.1×10^{-3}	2.1×10^{-3}
4	2.3×10^{-4}	5.0×10^{-4}	-2.5×10^{-4}	-2.6×10^{-5}	4.5×10^{-4}	4.6×10^{-4}

[a] Sum of the four terms. [b] Transition moment results from the interpolated DMF, used to show the accuracy of the separation.

as seen in Figure 6. As noted earlier, the *y* portion is negligible and the *z* portion is much greater than the *x* portion. Comparing the values between the conformers, it was found that while the *x* transition moment is slightly greater for the gauche isomer, the *z* transition moment is much greater for the trans isomer and summing the two components the trans isomer has a greater absorption. Therefore, we will be examining the difference in the *z* transition moment of the rotational conformers. To understand the reason for this feature, we separated the *z* transition moment into their dependence on the linear and nonlinear terms of the *z*-DMF, as was done in the previous paper[7] on 1,2-dichloroethylene. In the following, we will discuss the results of ethanol (Et), 2,2,2-trifluoroethanol, and 2-propanol separately.

By fitting the 16 single-point results onto a polynomial of bond displacement $R(R = r - r_{eq}$ in bohr) using the "Fit[data, function]" function built in the *Mathematica* program, we obtained the following:

$$\mu_z(trans\text{-Et}) \cong \mu_z(trans\text{-Et}, r_{eq}) + (3.46 \times 10^{-1})R^1 - (3.17 \times 10^{-1})R^2 - (1.34 \times 10^{-1})R^3 + (4.67 \times 10^{-2})R^4 \quad (6)$$

$$\mu_z(gauche\text{-Et}) \cong \mu_z(gauche\text{-Et}, r_{eq}) + (3.05 \times 10^{-1})R^1 - (2.68 \times 10^{-1})R^2 - (1.20 \times 10^{-1})R^3 + (4.31 \times 10^{-2})R^4 \quad (7)$$

in debye unit. Using these results and the matrix element of $\langle 0|R^n|v\rangle$, where the $|v\rangle$ denotes the vth vibrational wave function, we divided the *z* transition moment into each component of C_nR^n term, where C_n is the coefficient of the R^n term in eqs 6 and 7. The integrated values of $C_n\langle 0|R^n|v\rangle$ for the fundamental and the first three overtones are listed in Table 7. The main contribution in the transition moment in two conformers can be attributed to the linear (R^1) and quadratic (R^2) terms. Because the calculated overlap between the corresponding v quantum wave functions of the two isomers deviates from unity by less than 10^{-3}, $\langle 0|R^n|\ v\rangle$ is almost identical for the two conformers, as listed in Table 8. Therefore, we must compare the coefficients C_1 and C_2 in eqs 6 and 7. It can be seen that in both isomers C_1 and C_2 have different signs, as mentioned before, and the trans isomer has a greater absolute value for both terms. For the fundamental transition moment, as discussed before, we have seen that the R term is dominant, whereas the R^2 term causes a slight decrease. This is because the values of $\langle 0|R^n|1\rangle$ for $n = 1$ and 2 in Table 8 have the same sign. The transition moment for trans is greater due to the large absolute value of C_1. As for the overtone transitions, the values of $\langle 0|R^n|v\rangle$ ($v \geq 2$) for $n = 1$ and 2 have opposite signs as do the coefficients C_1 and C_2. Thereby, we see that the R^1 and R^2 terms of the transition moment have the same sign and add up to give the trans isomer a greater value compared to the gauche isomer.

TABLE 8: Integrated Value of $\langle 0|R^n|v\rangle$(bohr^n) for Ethanol

v	R^1	R^2	R^3	R^4
		trans		
1	1.3×10^{-1}	1.3×10^{-2}	7.8×10^{-3}	1.7×10^{-3}
2	1.5×10^{-2}	-2.2×10^{-2}	-4.3×10^{-3}	-3.1×10^{-3}
3	2.8×10^{-3}	-6.1×10^{-3}	3.9×10^{-3}	1.1×10^{-3}
4	7.3×10^{-4}	-1.9×10^{-3}	2.0×10^{-3}	-6.1×10^{-4}
		gauche		
1	1.3×10^{-1}	1.4×10^{-2}	7.9×10^{-3}	1.7×10^{-3}
2	1.5×10^{-2}	-2.2×10^{-2}	-4.3×10^{-3}	-3.1×10^{-3}
3	2.9×10^{-3}	-6.2×10^{-3}	3.9×10^{-3}	1.1×10^{-3}
4	7.5×10^{-4}	-1.9×10^{-3}	2.0×10^{-3}	-6.1×10^{-4}

For the *z*-DMF of 2,2,2-trifluoroethanol (TFEt), we obtain the following polynomial of bond displacement:

$$\mu_z(trans\text{-TFEt}) \cong \mu_z(trans\text{-TFEt}, r_{eq}) + (5.18 \times 10^{-1})R^1 - (2.24 \times 10^{-1})R^2 - (1.29 \times 10^{-1})R^3 + (3.02 \times 10^{-2})R^4 \quad (8)$$

$$\mu_z(gauche\text{-TFEt}) \cong \mu_z(gauche\text{-TFEt}, r_{eq}) + (4.85 \times 10^{-1})R^1 - (1.69 \times 10^{-1})R^2 - (1.06 \times 10^{-1})R^3 + (2.87 \times 10^{-2})R^4 \quad (9)$$

and for 2-propanol (Pr), we obtain the following:

$$\mu_z(trans\text{-Pr}) \cong \mu_z(trans\text{-Pr}, r_{eq}) + (2.65 \times 10^{-1})R^1 - (3.00 \times 10^{-1})R^2 - (1.23 \times 10^{-1})R^3 + (4.28 \times 10^{-2})R^4 \quad (10)$$

$$\mu_z(gauche\text{-Pr}) \cong \mu_z(gauche\text{-Pr}, r_{eq}) + (2.53 \times 10^{-1})R^1 - (2.48 \times 10^{-1})R^2 - (1.10 \times 10^{-1})R^3 + (3.95 \times 10^{-2})R^4 \quad (11)$$

in debye units. Once again it can be noticed that C_1 and C_2 are of opposite signs and the trans isomer has a greater absolute value. Correspondingly, in Figure 7, the *z* direction DMF of the trans isomer has a slightly acute curve than the one for the gauche isomer. The same trend can also be seen for 1-propanol in Tables 4 and 6, where the absorption intensities of the "T" labeled isomers are greater than the ones labeled with "G". As a conclusion, the difference in the sign of the first and second derivative terms along with the greater absolute value of the two terms in the *z*-DMF were responsible for the stronger absorption intensity in the trans conformer.

4. Conclusion

We calculated the fundamental and overtone spectra of the OH stretching vibration of nitric acid, trifluoroacetic acid, acetic acid, 2,2,2-trifluoroethanol, methanol, ethanol, 1-propanol,

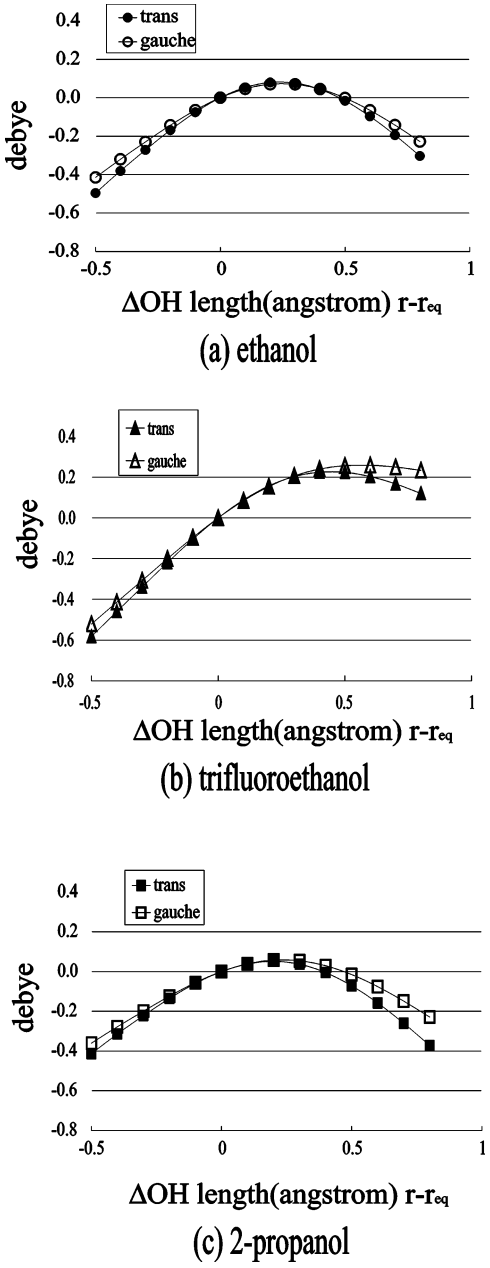

Figure 7. Deviation of the *z* component of the dipole moment function of (a) ethanol, (b) 2,2,2-trifluoroethanol, and (c) 2-propanol.

2-propanol, *tert*-butyl alcohol, and the OH radical. Under the local mode model, we were able to obtain accurate vibrational spectra of the fundamental and overtone transitions using a high precision vibrational calculation along with the PES and three-dimensional DMF calculated from quantum chemical calculations. For the fundamental transition, we investigated the difference between the local and normal mode vibrational calculation results. For the overtone absorption intensity, we found that the contribution from the DMF in the direction parallel to the OH bond and the one perpendicular to the OH bond were different between the acids and alcohols. However, as a sum, the alcohols and the acids give similar absorption intensities. For alcohols with rotational conformers, such as ethanol and propanol, we found that the isomer with the alkyl group in the trans position of the vibrating OH bond has a greater transition energy and a stronger absorption intensity. The larger value of absorption intensity in the trans isomer is attributed to the difference in the sign of the linear term and the quadratic term along with the greater absolute value in both terms for the DMF in the direction parallel to the OH bond.

Acknowledgment. This work was supported in part by Research and Development Applying Advanced Computational Science and Technology, Japan Science and Technology Corporation, and by Grants-in-Aids for Scientific Research and for the 21st Century COE program "KEIO LCC" both from the Ministry of Education, Science, Culture, and Sports of Japan. K.T. would like to thank professor James A. Phillips for the information on the experimental details.

Supporting Information Available: Tables of the calculated single-point results of the potential energy and the dipole moment at the B3LYP/6-311++G(3df,3pd) level of theory for all of the molecules mentioned in this paper. This material is available free of charge via the Internet at http://pubs.acs.org.

References and Notes

(1) Swofford, R. L.; Long, M. E.; Albrecht, A. C. *J. Chem. Phys.* **1976**, *65*, 179.
(2) Henry, B. R. *Acc. Chem. Res.* **1977**, *10*, 207.
(3) Child, M. S.; Lawton, R. T. *Chem. Phys. Lett.* **1982**, *87*, 217.
(4) Lewerenz, M.; Quack, M. *Chem. Phys. Lett.* **1986**, *123*, 197.
(5) Low, G. R.; Kjaergaard, H. G. *J. Chem. Phys.* **1999**, *110*, 9104.
(6) Fedorov, A. V.; Snavely, D. L. *Chem. Phys.* **2000**, *254*, 169.
(7) Takahashi, K.; Sugawara, M.; Yabushita, S. *J. Phys. Chem. A* **2002**, *106*, 2676.
(8) Lin, H.; Yuan, L.-F.; He, S.-G.; Wang, X.-G. *J. Chem. Phys.* **2001**, *114*, 8905.
(9) Lin, H.; Bürger, H.; MKadmi, E. B.; He, S.-G.; Yuan, L.-F.; Breidung, J.; Thiel, W.; Huet, T. R.; Demaison, J. *J. Chem. Phys.* **2001**, *115*, 1378.
(10) Donaldson, D. J.; Tuck, A. F.; Vaida, V. *Chem. Rev.*, in press.
(11) Chỳlek, P.; Geldart, D. J. W. *Geophys. Res. Lett.* **1997**, *24*, 2015.
(12) Donaldson, D. J.; Frost, G. J.; Rosenlof, K. H.; Tuck, A. F.; Vaida, V. *Geophys. Res. Lett.* **1997**, *24*, 2651.
(13) Reynard, L. M.; Donaldson, D. J. *J. Phys. Chem. A* **2002**, *106*, 8651.
(14) Lange, K. R.; Wells, N. P.; Plegge, K. S.; Phillips, J. A. *J. Phys. Chem. A* **2001**, *105*, 3481.
(15) Becke, A. D. J. *Chem. Phys.* **1993**, *98*, 5648.
(16) Lee, C.; Yang, W.; Parr, R. G. *Phys. Rev. B* **1988**, *37*, 785.
(17) McLean, A. D.; Chandler, G. S. *J. Chem. Phys.* **1980**, *72*, 5639.
(18) Krishnan, R.; Binkley, J. S.; Seeger, R.; Pople, J. A. *J. Chem. Phys.* **1980**, *72*, 650.
(19) Clark, T.; Chandrasekhar, J.; Spitznagel, G. W.; Schleyer, P. v. R. *J. Comput. Chem* **1983**, *4*, 294.
(20) Frisch, M. J.; Pople, J. A.; Binkley, J. S. *J. Chem. Phys.* **1984**, *80*, 3265.
(21) Frisch, M. J.; Trucks, G. W.; Schlegel, H. B.; Scuseria, G. E.; Robb, M. A.; Cheeseman, J. R.; Zakrzewski, V. G.; Montgomery, J. A., Jr.; Stratmann, R. E.; Burant, J. C.; Dapprich, S.; Millam, J. M.; Daniels, A. D.; Kudin, K. N.; Strain, M. C.; Farkas, O.; Tomasi, J.; Barone, V.; Cossi, M.; Cammi, R.; Mennucci, B.; Pomelli, C.; Adamo, C.; Clifford, S.; Ochterski, J.; Petersson, G. A.; Ayala, P. Y.; Cui, Q.; Morokuma, K.; Malick, D. K.; Rabuck, A. D.; Raghavachari, K.; Foresman, J. B.; Cioslowski, J.; Ortiz, J. V.; Stefanov, B. B.; Liu, G.; Liashenko, A.; Piskorz, P.; Komaromi, I.; Gomperts, R.; Martin, R. L.; Fox, D. J.; Keith, T.; Al-Laham, M. A.; Peng, C. Y.; Nanayakkara, A.; Gonzalez, C.; Challacombe, M.; Gill, P. M. W.; Johnson, B. G.; Chen, W.; Wong, M. W.; Andres, J. L.; Head-Gordon, M.; Replogle, E. S.; Pople, J. A. *Gaussian 98*, revision A.5; Gaussian, Inc.: Pittsburgh, PA, 1998.
(22) Skeel, R. D.; Keiper, J. D. *Elementary Numerical Computing with Mathematica*; McGraw-Hill: New York, 1993; Chapter 5.
(23) Atkinson, K. *Elementary Numerical Analysis*; John Wiley and Sons: New York, 1985; Chapter 5.
(24) McCullough, E. A., Jr; Wyatt, R. E. *J. Chem. Phys.* **1971**, *54*, 3578.
(25) Cerjan, C.; Kulander K. C. *Comput. Phys. Commun.* **1991**, *63*, 529.
(26) These figures were drawn using the MOLDEN 3.6 program, obtained via Internet:http://www.cmbi.kun.nl/schaft/molden/molden.html.
(27) Phillips, J. A. Private communication.
(28) Kakar, R. K.; Quade, C. R. *J. Chem. Phys.* **1980**, *72*, 4300.
(29) Durig, J. R.; Bucy, W. E.; Wurrey, C. J.; Carreira, L. A. *J. Phys. Chem.* **1975**, *79*, 988.
(30) Fang, H. L.; Swofford, R. L. *Chem. Phys. Lett.* **1984**, *105*, 5.

(31) Alsenoy, C. V.; Scarsdale, J. N.; Willliams, J. O.; Schäfer, L. *J. Mol. Struct.* **1982**, *86*, 365.
(32) Weibel, J. D.; Jackels C. F.; Swofford R. L. *J. Chem. Phys.* **2002**, *117*, 4245.
(33) Donaldson, D. J.; Orlando, J. J.; Amann, S.; Tyndall, G. S.; Proos, R. J.; Henry, B. R.; Vaida, V. *J. Phys. Chem. A* **1998**, *102*, 5171.
(34) Kagarise, R. E. *J. Chem. Phys.* **1957**, *27*, 519.
(35) Maillard, J. P.; Chauville, J.; Mantz, A. W. *J. Mol. Spectrosc*. **1976**, *63*, 120.
(36) Cox, A. P.; Riveros, J. M. *J. Chem. Phys.* **1965**, *42*, 3106.
(37) Computational Chemistry Comparison and Benchmark DataBase, via Internet: http://srdata.nist.gov/cccbdb.
(38) Culot, J. P. Fourth Austin Symposium on Gas-Phase Molecular Structure, Austin, TX, 1972.
(39) Huber, K. P.; Hertzberz, G. *Molecular Spectra and Molecular Structure IV. Constants of Diatomic Molecules*; Van Nostrand Reinhold Co.: New York, 1979.
(40) Fang, H. L.; Compton, D. A. C. *J. Phys. Chem*. **1988**, *92*, 6518.
(41) Henry, B. R. *Acc. Chem. Res.* **1987**, *20*, 429.
(42) Ha, T.-K.; Lewerentz, M.; Marquardt, R.; Quack, M. *J. Chem. Phys.* **1990**, *93*, 7097.
(43) Medvedev, E. S. *J. Chem. Phys.* **1996**, *108*, 81.
(44) Lehmann, K. K.; Smith, A. M. *J. Chem. Phys.* **1990**, *93*, 6140.
(45) Amrein, A.; Dübal, H.-R.; Lewerenz, M.; Quack, M. *Chem. Phys. Lett.* **1984**, *112*, 387.
(46) Burberry, M. S.; Albrecht, A. C. *J. Chem. Phys.* **1979**, *71*, 4768.
(47) Xu, S.; Liu, Y.; Xie, J.; Sha, G.; Zhang, C. *J. Phys. Chem. A* **2001**, *105*, 6048.
(48) Krueger, P. J.; Jan, J.; Wieser, H. *J. Mol. Struct.* **1970**, *5*, 375.
(49) Reed, A. E.; Schleyer, P. v. R. *J. Am. Chem. Soc.* **1987**, *109*, 7362.
(50) Omoto, K.; Marusaki, K.; Hirao, H.; Imade, M.; Fujimoto, H. *J. Phys. Chem. A* **2000**, *104*, 6499.